Analog and Successive Channel Equalization in Strong Line-of-Sight MIMO Communication

Xiaohang Song*, Wolfgang Rave*, and Gerhard Fettweis*§

* Vodafone Chair, Technische Universität Dresden, Dresden, Germany,
Email: {xiaohang.song, wolfgang.rave, gerhard.fettweis}@tu-dresden.de

***Abstract*—In this work, we show a new design of analog equalizing network for N-stream strong Line-of-Sight MIMO communication, aiming at improved robustness. The design includes a core fixed equalizing network that equalizes ideal spatially orthogonal channels. Existing works show that the fixed equalizing network can equalize a spatially orthogonal MIMO system with parallel arrays. However, it is observed that such a fixed equalizing network is very sensitive to displacement errors. To make the system robust, state-of-the-art approaches use N^2 fully controlled analog elements to perfectly equalize the channel via aligning the structured interferences. In this work, the terms causing the sensitiveness of fixed analog equalizing networks are identified. By compensating the tackled sensitive terms, the proposed design uses only $2N$ fully controlled analog elements and the robustness of the system is improved significantly. Meanwhile, by exploring the channel property, this work shows that if the spatially orthogonality is achieved by uniform rectangular arrays, the equalization can be applied with a new two-stage scheme. The scheme can be applied to spatially orthogonal MIMO systems with digital and/or analog equalization. Meanwhile, the computational complexity, required components number, as well as the complexity of the hardware design are significantly reduced.**

I. Introduction

In 2020-2030, peak data rates in cellular networks are expected to be in the order of 10 $\mathrm{Gb/s}$ [1]. Base stations will serve multiple sectors and will be no more than 100 m apart in urban areas. Previous work [2] showed the great potential in building ultra high speed fixed wireless backhaul links to meet the growing demand for high capacity of the front/back-haul. For future dense networks, wireless front/back-haul links offer easy and cheap deployment in comparison with costly optical fibers. The unlicensed 60 GHz band has become most popular for this purpose due to available large bandwidth, high frequency reuse and reasonable array sizes which can fully exploit the spatial multiplexing gains in *Line-of-Sight* (LoS) channels. The works in [3], [4], [5] have given the solution to the optimized spatial arrangements on parallel planes that provide the MIMO channel matrices with orthogonality. However, full spatial multiplexing can also be achieved with arrangements on tilted non-parallel planes [6], [7], [8], [9] or even more complicated 3D arrangements [9]. Furthermore, [5] showed high robustness of the spatial multiplexing gain in LoS MIMO against degradations like translation and rotation.

§This work has been supported by the German Research Foundation (DFG) in the framework of priority program SPP 1655 "Wireless Ultra High Data Rate Communication for Mobile Internet Access".

Lots of works in strong LoS systems consider short range communication. In those cases, hardware can be fabricated almost perfectly according to the rules of optimal arrangement as mentioned before. Therefore, the phase relations in a MIMO channel are known even without channel measurements and analog components can be used for channel equalization. A fixed analog equalizing network can perfectly separate the structurally interfered streams before the *Analog-to-Digital Converters* (ADCs). [10] investigated the channel capacity degradation if non-ideal analog components with amplitude errors and phase errors are involved in a fixed equalizing networks. [11] provides experimental evaluation of a 2×2 LoS MIMO system with a fixed analog equalizing network. Due to the fact that the streams can be separated before quantization, the dynamic is reduced, and the energy efficiency of the ADCs is improved significantly as the ADCs are already very power hungry at high sampling rates.

Due to the fact that applications like wireless backhaul with LoS MIMO channels are also highly deterministic, the channel parameters, as well as the equalization matrix, do not change rapidly with respect to time. However, displacement always happen during manufacturing and deployment in practical systems. Works in [12], [13] demonstrated a channel equalizing network for 2×2 LoS MIMO systems with phase shifters operating at intermediate frequencies. They demonstrate LoS MIMO systems with analog equalizing networks that provide communication at distances like 6 meter range in an indoor environment and 41 meter range in an outdoor environment. If the channel is deterministic and ideal phase relations are known, a fixed network should work perfectly in case of optimal arrangements. However, within their work they mentioned that they still have to manually adjust phases to null the cross-channel interference in a practical system due to the phase variation. It is shown by our work that the phase relations are very sensitive to displacement in practice. Their work was extended to a 4×4 MIMO system [14]. Meanwhile, in order to compensate the phase variation and achieve robustness in practical systems, variable gain amplifiers allowing magnitude scaling and phase shift operations on baseband signals are used for every path inside the analog equalizing network. A CMOS based phase shifter design for 60GHz is presented in [15]. The proposed agile linear phase shifter consumes 10mV in their test. Although the power consumption is in general smaller that ADCs, the number of linear phase shifters should also be

978-1-4799-6664-6/16/$31.00 ©2016 IEEE

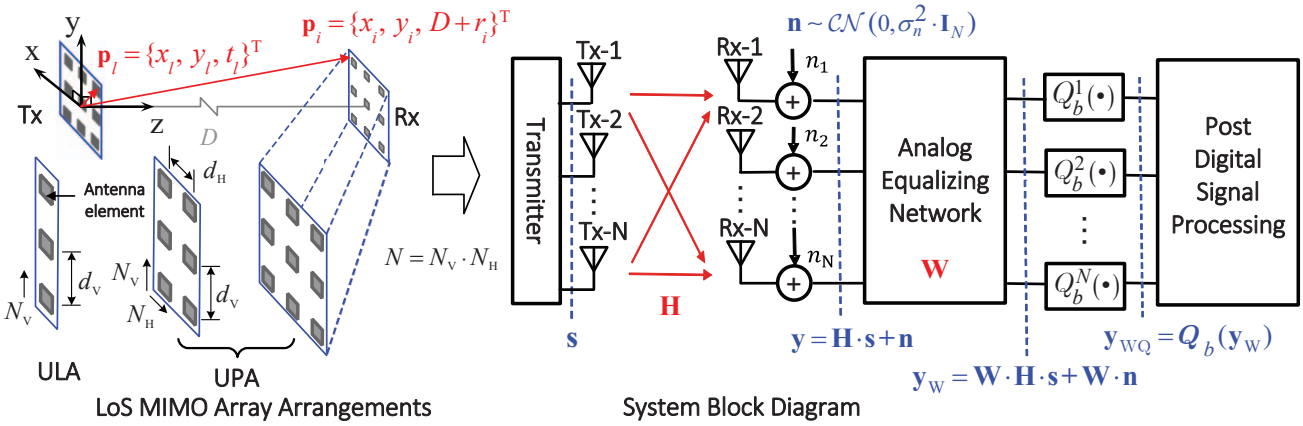

Fig. 1: System model.

limited and it should not be used on every path of an analog equalizing network. As shown in [9], phase variations are actually strongly correlated. In this work we show that those phase variation can be compensated easily with a significantly lower number of fully controlled elements. This work is also closely related to our work in [16]. In that work, a detailed study of the proposed analog equalization design is carried out focusing on its impact on digital processing where only low resolution ADCs are used.

The paper is organized as follows. In Section II, we introduce the system model of the analog equalizing network combined with LoS MIMO systems as well as some basic properties of the channel. In Section III, we propose a new analog equalizing network design considering a fixed equalizing network with phase adjustment. Furthermore, a new two-stage fixed equalizing network is proposed for simplifying the complexity of the fixed equalizing network design in this section. In Section IV, the mutual information is proposed as evaluation criteria for the system performance. In Section V, numerical evaluations are applied to show that the sensitiveness of the fixed analog equalizing network matches our prediction. Therefore, higher robustness is provided by the proposed network design with phase adjustment that compensates the sensitive items. Finally, our work is concluded in Section VI.

II. System Model

Fig. 1 shows a symmetric $N \times N$ LoS MIMO transmission system. To simplify the description of the system, we split the system into three parts as channel model, analog equalization and analog-to-digital conversion.

A. Channel Model

Considering a LoS MIMO system with transmit distance D which is much larger than the inter antenna distances d_{V} and d_{H}, the receive vector in a frequency flat strong LoS MIMO channel is modeled as

$$\mathbf{y} = \mathbf{H} \cdot \mathbf{s} + \mathbf{n}, \tag{1}$$

where $\mathbf{n}$ is i.i.d. zero mean complex white Gaussian noise in base-band with $\mathbf{n} \sim \mathcal{CN}(\mathbf{0}, \sigma_n^2 \cdot \mathbf{I}_N)$. $\mathbf{s}$ is the transmit vector with total transmit power P_{T}, $\mathbb{E}(\mathbf{s}^{\mathrm{H}}\mathbf{s}) \leq P_{\mathrm{T}}$. Due to the fact that the power attenuation factors between different antenna pairs are almost the same under assumption that $D \gg d_{\mathrm{V}}$, d_{H}, we neglect the power differences [2]. By $\mathbf{H} \in \mathbb{C}^{N \times N}$ we denote the phase coupling matrix in the strong LoS MIMO channel with entries

$$h_{il} \triangleq e^{-j\frac{2\pi}{\lambda}D_{il}}, \tag{2}$$

where D_{il} denotes the transmit distance between transmit antenna l and received antenna i. λ is the wavelength of the carrier frequency.

To simplify the later discussion, we assume that the transmitted signals in all N data streams follow the same K-QAM modulation with K constellation points given as $\mathbb{A} = \{\mathscr{A}_1, \mathscr{A}_2, \ldots, \mathscr{A}_K\}$. Therefore, the transmit vector $\mathbf{s}$ belongs to a N-dimensional discrete space $\mathbb{M} = \mathbb{A}^N$, where $\mathbb{M} = \mathbb{A}^N$ is a finite set containing all possible transmit vectors $\boldsymbol{\mathcal{S}}$s.

For simplicity, we consider one antenna l of transmit antenna array ($\mathrm{T_x}$) and one antenna i of receive antenna array ($\mathrm{R_x}$). Additionally, we assume that the phase center of the transmitter antenna array is located at (0, 0, 0) and the transmit direction is along the z-axis. Therefore, the phase center of the receive antenna is located at (0, 0, D). The position of the antennas l and i can be described by the vectors

$$\mathbf{p}_l = \{x_l, y_l, t_l\}^{\mathrm{T}}, \quad \mathbf{p}_i = \{x_i, y_i, D + r_i\}^{\mathrm{T}}, \tag{3}$$

where we assume that the additional offsets t_l, r_i along the transmit direction and the antenna aperture, the area of the projection of the array in the xy-plane, are much smaller than the transmit distance, i.e. $x_l, y_l, t_l, x_i, y_i, r_i \ll D$. The antenna distance D_{il} between antennas l and i, which determines the entries of the channel matrix and ultimately the link performance according to Equation (2), can be written as

$$\begin{aligned} D_{il} &= |\mathbf{p}_i - \mathbf{p}_l|_2 \\ &= \sqrt{(x_i - x_l)^2 + (y_i - y_l)^2 + (D + r_i - t_l)^2} \\ &\approx D + r_i - t_l + \frac{(x_i - x_l)^2}{2D} + \frac{(y_i - y_l)^2}{2D}. \end{aligned} \tag{4}$$

The approximation in Equation (4) follows by a first order Taylor expansion of the square root using $x_l, y_l, t_l, x_i, y_i, r_i \ll D$. More details of the deviation were given in [9]. Without loss

of generality, the phase shift caused by D can be dropped as it is a constant for all paths. Then the channel coefficient in Equation (2) can be factorized as

$$h_{il} \propto e^{-j\frac{2\pi}{\lambda}r_i} e^{-j\frac{2\pi}{\lambda}\frac{(x_i-x_l)^2}{2D}} e^{-j\frac{2\pi}{\lambda}\frac{(y_i-y_l)^2}{2D}} e^{j\frac{2\pi}{\lambda}t_l}. \quad (5)$$

By separating phase shifts due to displacement along z- and xy-axes among the antennas, the channel matrix $\mathbf{H}$ can directly be decomposed into

$$\mathbf{H} = \mathbf{D}_{\parallel,\mathrm{r}} \cdot \mathbf{H}_{\perp} \cdot \mathbf{D}_{\parallel,\mathrm{t}}, \quad (6)$$

where $\mathbf{D}_{\parallel,\mathrm{t}}$, $\mathbf{D}_{\parallel,\mathrm{r}}$ are diagonal matrices that represent the phase shifts caused by the offsets along the transmit direction at $\mathrm{T_x}$ and $\mathrm{R_x}$, respectively. Their diagonal entries are $\{\mathbf{D}_{\parallel,\mathrm{t}}\}_{ll} \triangleq e^{j\frac{2\pi t_l}{\lambda}}$, $\{\mathbf{D}_{\parallel,\mathrm{r}}\}_{ii} \triangleq e^{-j\frac{2\pi r_i}{\lambda}}$, $i,l \in [1,N]$. $\mathbf{H}_{\perp}$ is the channel matrix contributed by the spatial multiplexing on the broadside relative to the transmit direction with $\{\mathbf{H}_{\perp}\}_{il} = e^{-j\frac{2\pi}{\lambda}\frac{(x_i-x_l)^2+(y_i-y_l)^2}{2D}}$.

Considering two parallel *Uniform Linear Arrays* (ULAs) or *Uniform Planar Arrays*, the special arrangements following the design in [5] can fully exploit the spatial multiplexing gain of LoS MIMO systems. The arrangements and the inter antenna spacing d_{V}, d_{H} mainly depend on the transmit distance D, wavelength λ and antenna number N. In symmetric cases, d_{V}, d_{H} satisfy $d_{\mathrm{V}} = \sqrt{\lambda D/N_{\mathrm{V}}}$ and $d_{\mathrm{H}} = \sqrt{\lambda D/N_{\mathrm{H}}}$, respectively. By choosing d_{V}, d_{H} appropriately and arranging the transceiver arrays in two parallel planes that are perpendicular to the transmit direction, $\mathbf{H}$ becomes the spatially orthogonal matrix $\mathbf{H}_{\mathrm{o}}$ with $\mathbf{H}_{\mathrm{o}}^{\mathrm{H}} \cdot \mathbf{H}_{\mathrm{o}} = N \cdot \mathbf{I}_N$. As an example, the entries of $\mathbf{H}_{\mathrm{o}}$ in an optimally arranged and symmetric system with parallel ULAs satisfy $\{\mathbf{H}_{\mathrm{o}}\}_{il} = e^{-j\pi(i-l)^2/N}$. When $N = 3$, $\mathbf{H}_{\mathrm{o}}$ becomes

$$\mathbf{H}_{\mathrm{o}} = \begin{bmatrix} 1 & e^{-j\frac{\pi}{3}} & e^{-j\frac{4\pi}{3}} \\ e^{-j\frac{\pi}{3}} & 1 & e^{-j\frac{\pi}{3}} \\ e^{-j\frac{4\pi}{3}} & e^{-j\frac{\pi}{3}} & 1 \end{bmatrix}. \quad (7)$$

As given by [9], any parallel, arbitrary rotated optimal planar arrays or even more complicated optimal arrays with 3D arrangements should satisfy $\mathbf{H}_{\perp} = \mathbf{H}_{\mathrm{o}}$. However, if there exists displacement of the optimal parallel arrangement, the phase coupling matrix $\mathbf{H}$ will have mismatches with $\mathbf{H} \neq \mathbf{H}_{\mathrm{o}}$ and $\mathbf{H}_{\perp} \neq \mathbf{H}_{\mathrm{o}}$.

B. Analog Equalization

An analog equalizing network, represented by a weighting matrix $\mathbf{W} \in \mathbb{C}^{N\times N}$, is introduced in the system for equalizing the vector received through a deterministic MIMO channel like in a strong LoS MIMO system. The weighted vector $\mathbf{y}_{\mathrm{W}}$ is then expressed as

$$\mathbf{y}_{\mathrm{W}} = \mathbf{W} \cdot \mathbf{y} = \mathbf{W} \cdot \mathbf{H} \cdot \mathbf{s} + \tilde{\mathbf{n}}, \quad (8)$$

where $\tilde{\mathbf{n}} = \mathbf{W} \cdot \mathbf{n}$. Ideally, in case of optimal arrangement $\mathbf{H} = \mathbf{H}_{\mathrm{o}}$, a fixed $\mathbf{W} = \mathbf{H}_{\mathrm{o}}^{\mathrm{H}}$ is capable of equalizing the channel, separating all streams and converting the multi-user detection problem into separate SISO channels.

C. Analog-to-Digital Conversion

After equalizing the channel, the signals are quantized and converted for digital-band processing. Assuming that transceivers are perfectly synchronized, the signals are split up into real and imaginary parts. These signals are fed to the inputs of two banks of quantizers $Q^{\mathrm{R}_1}, Q^{\mathrm{R}_2}, \ldots, Q^{\mathrm{R}_N}$ for the real and $Q^{\mathrm{I}_1}, Q^{\mathrm{I}_2}, \ldots, Q^{\mathrm{I}_N}$ for the imaginary parts of different data streams $l \in \{1, 2, \ldots, N\}$. To simplify the discussion in the rest of the paper, we assume all of the above mentioned quantizers to be of same type[1] and denote them as $Q_b^{\alpha}(x)$ with $\alpha \in \{\mathrm{R}_1, \mathrm{R}_2, \ldots, \mathrm{R}_N\} \bigcup \{\mathrm{I}_1, \mathrm{I}_2, \ldots, \mathrm{I}_N\}$. Here, b denotes the number of bits that are used for representing the ADC outputs. The input-output relationship $Q_b^{\alpha}(x)$ of the ADC Q^{α} is defined for voltages x by

$$Q_b^{\alpha}(x) = \begin{cases} q_1^{\alpha} & \text{if} \quad -\infty < x \leq x_1^{\alpha} \\ q_2^{\alpha} & \text{if} \quad x_1^{\alpha} < x \leq x_2^{\alpha} \\ \vdots & \vdots \qquad\qquad \vdots \\ q_{2^b}^{\alpha} & \text{if} \quad x_{2^b-1}^{\alpha} < x < +\infty \end{cases}, \quad (9)$$

where the $\{q_1^{\alpha}, q_2^{\alpha}, \ldots, q_{2^b}^{\alpha}\}$ and $\{x_1^{\alpha}, x_2^{\alpha}, \ldots, x_{2^b-1}^{\alpha}\}$ are the sets of quantization values and their thresholds, respectively.

Combining the outputs of the real and imaginary parts of the quantizers, the quantizing operation $Q_b^l(z)$ on the complex constellation plane can be written as

$$Q_b^l(z) = Q_b^{\mathrm{R}_l}[\Re(z)] + j \cdot Q_b^{\mathrm{I}_l}[\Im(z)], \quad (10)$$

where $\Re(z)$, $\Im(z)$ indicate the real and imaginary parts of the complex number z.

Now, we write the input-output relationship of the analog-to-digital conversion as

$$\mathbf{y}_{\mathrm{WQ}} = \mathbf{Q}_b(\mathbf{y}_{\mathrm{W}}) \in \mathbb{Q}, \quad (11)$$

where $\mathbb{Q}$ denotes a finite set containing all possible outputs of the quantizers.

III. Analog equalizing network

In optimal arrangements, as mentioned above, phase coupling matrices are orthogonal matrices with entries having unit modulus. Therefore, the weighting matrix $\mathbf{W}$ can be realized with entries having unit modulus, e.g. $\mathbf{W} = \mathbf{H}_{\mathrm{o}}^{\mathrm{H}}$ and $\mathbf{H}_{\mathrm{o}}^{\mathrm{H}} \cdot \mathbf{H}_{\mathrm{o}} = N \cdot \mathbf{I}_N$. Later in the discussion, the phase coupling vector for the l-th transmit antenna is modeled as $\mathbf{h}_{\mathrm{o},l}$ which is the l-th column of matrix $\mathbf{H}_{\mathrm{o}}$. Considering this, the spatially orthogonal channel can be fully equalized using an analog filter network with different delays or phase shifters. The analog equalizing network constructs new weighted vectors by aligning the received signals from different receive antennas. The alignment brings performance improvement by separating one signal from the interference of the others.

The block diagram of the analog equalizing network is illustrated in Fig. 2. To simplify the diagram, we omit units for signal synchronization or carrier frequency down-conversion.

[1]Quantizers at different data streams may not be identical to each other, if quantization are applied on signals with different scales or different distributions of amplitudes.

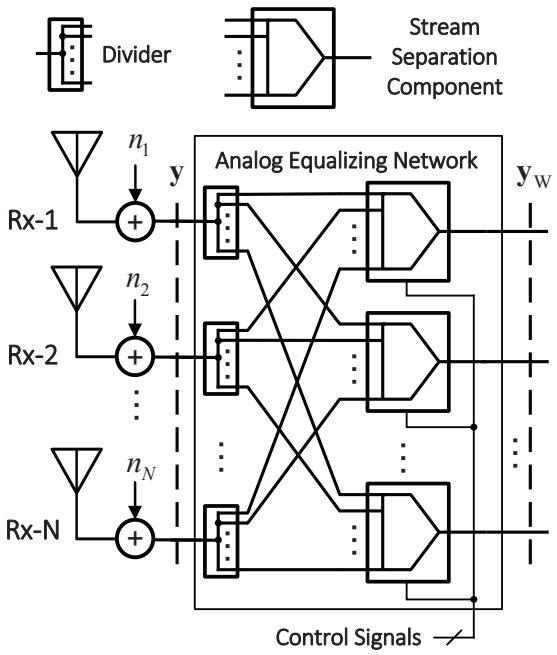

Fig. 2: Analog equalizing network block diagram.

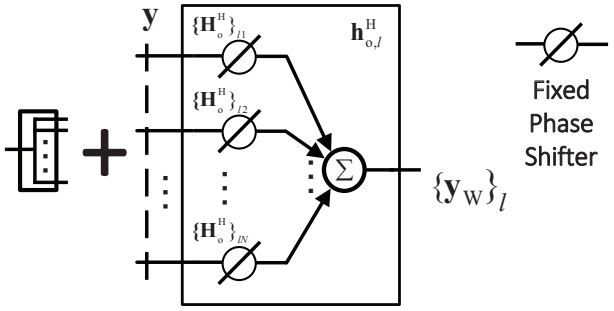

Fig. 3: Stream separation design with fixed phase shifts only for perfectly arranged arrays with low robustness against displacements.

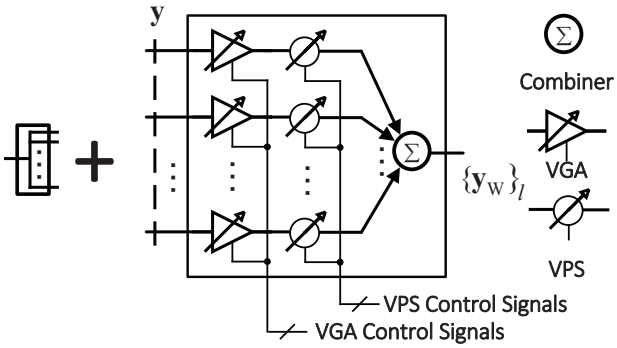

Fig. 4: Stream separation design with perfect stream equalization but complex system design. $\{\mathbf{y}_\mathrm{W}\}_l$ indicates the l-th entry in weighted vector $\mathbf{y}_\mathrm{W}$.

We focus on the phases and amplitudes of the baseband signals. The signal from each receive antenna is split into N copies by a divider. Afterwards, every stream separation component combines the copies from all received signals. By applying different phase shifts to signals with unit magnitude, the stream separation component reconstructs the transmitted signals of the corresponding transmit antenna.

The works in [10], [11] used fixed analog equalizing networks with $\mathbf{W} = \mathbf{H}_\mathrm{o}^\mathrm{H}$ as sketched in Fig. 3 assuming ideal positions. As will be shown in Section V, a fixed analog equalizing network is very sensitive to displacements. In case of displacements, especially the non-equivalent displacements along the transmit direction, all the N^2 entries within $\mathbf{H}$ change rapidly which makes the performance of a fixed equalizing network $\mathbf{W} = \mathbf{H}_\mathrm{o}^\mathrm{H}$ very sensitive. Therefore, experimental systems as in [14] used N^2 fully controlled *Variable Gain Amplifiers* (VGAs) and *Variable Phase Shifters* (VPSs), as sketched in Fig. 4, to equalize the almost deterministic channel without giving the explanations of sensitiveness or robustness. As will be explained in this section, the dominant errors of $\mathbf{H}$ come from $\mathbf{D}_{\parallel,\mathrm{r}}$ and $\mathbf{D}_{\parallel,\mathrm{t}}$ in Equation (6). Therefore, we propose a new design combining a fixed equalizing network with phase adjustment on different streams only as shown in Fig. 5.

A. Fixed stream separation with Phase Adjustment Design

As shown by P. Larsson in [5], with perfect equalization the spatial multiplexing gain is quite robust w.r.t displacements. Only for rather large displacements, the undesired interferences become large and spatial multiplexing gains decrease. Therefore, having the channel perfectly equalized with very complicated hardware design and high running costs may not bring the gain worth the costs within the allowed displacements in practical systems. Meanwhile, by examining Equation (5), it can be seen that the entries of the channel are very sensitive to offset *differences* along the transmit direction due to the fact that the errors are measured in unit of λ instead of $\sqrt{\lambda D}$ for in-plane ($xy-$plane) errors. Hence, we suggest in this paper a fixed analog network with fewer controllable elements. The number of fully controlled VPSs is reduced from N^2 to $2N$ and it is not necessary to implement VGAs. In case of gain mismatches due to dirty RF issues, N VGAs are capable of compensating unequal amplitudes.

The proposed stream separation components consist of three stages as shown in Fig. 5 for a single data stream l. The first stage applies phase shifts before the divider and compensates $\mathbf{D}_{\parallel,\mathrm{r}}$ caused by displacements in transmit direction for better robustness. The second stage consists of a fixed stream separation component $\mathbf{f}_l^\mathrm{T} = \mathbf{h}_{\mathrm{o},l}^\mathrm{H}$ with fixed phase shifters or delay lines that can perfectly separate the l-th channel in case of optimal arrangements. The third stage consists of a VPS with phase shift ϕ_l. The VPS compensates the remaining phase shift on the desired signal. In case of an optimal antenna arrangement with parallel antenna arrays, $\mathbf{f}_l^\mathrm{T} \cdot \mathbf{h}_{\mathrm{o},i} = N \cdot \delta_{il}$ and $\phi_l = 0$, where δ_{il} indicates the Kronecker delta.

Considering displacements of the optimal arrangements involving translations and rotations, the phase coupling $\mathbf{H}_\perp$ is different from $\mathbf{H}_\mathrm{o}$ by $\Delta\mathbf{H}$ and therefore the channel matrix $\mathbf{H}$ is modeled as

$$\mathbf{H} = \mathbf{D}_{\parallel,\mathrm{r}} \cdot \underbrace{(\mathbf{H}_\mathrm{o} + \Delta\mathbf{H})}_{\mathbf{H}_\perp} \cdot \mathbf{D}_{\parallel,\mathrm{t}}. \tag{12}$$

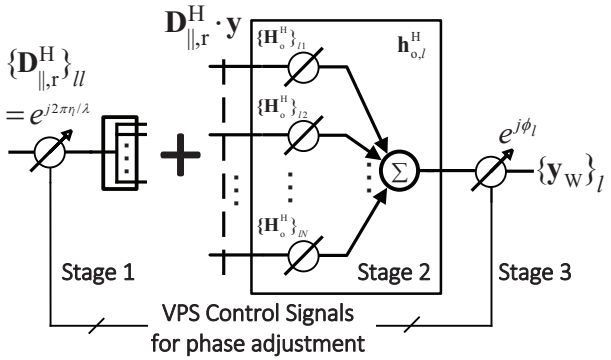

Fig. 5: Fixed stream separation with phase adjustment design.

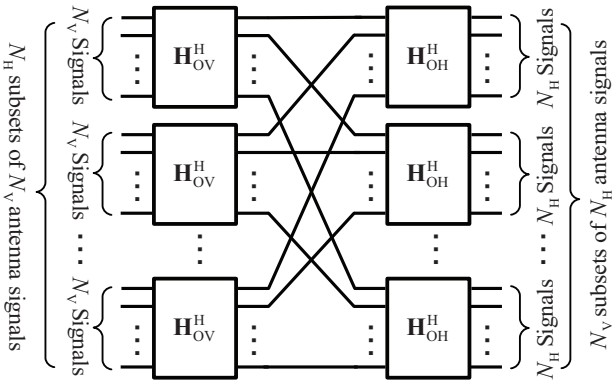

Fig. 6: A two-stage fixed analog equalizing network design.

The filtered signal of the l-th data steam after analog filtering satisfies

$$\begin{aligned} y_{\mathrm{F},l} &= \mathbf{f}_l^{\mathrm{T}} \cdot \mathbf{D}_{\parallel,\mathrm{r}}^{\mathrm{H}} \cdot \mathbf{y} \\ &= \mathbf{f}_l^{\mathrm{T}} \cdot [(\mathbf{H}_{\mathrm{o}} + \Delta\mathbf{H}) \cdot \mathbf{D}_{\parallel,\mathrm{t}} \cdot \mathbf{s} + \mathbf{D}_{\parallel,\mathrm{r}}^{\mathrm{H}} \cdot \mathbf{n}] \\ &= (N \cdot \mathbf{e}_l^{\mathrm{T}} + \mathbf{f}_l^{\mathrm{T}} \cdot \Delta\mathbf{H}) \cdot \mathbf{D}_{\parallel,\mathrm{t}} \cdot \mathbf{s} + \mathbf{f}_l^{\mathrm{T}} \cdot \mathbf{D}_{\parallel,\mathrm{r}}^{\mathrm{H}} \cdot \mathbf{n} \\ &= \underbrace{(N + \mathbf{f}_l^{\mathrm{T}} \cdot \Delta\mathbf{h}_l) \cdot e^{j\frac{2\pi t_l}{\lambda}} \cdot s_l}_{\text{Desired signal}} + \underbrace{\sum_{p=1, p\neq l}^{N} \mathbf{f}_l^{\mathrm{T}} \cdot \Delta\mathbf{h}_p \cdot e^{j\frac{2\pi t_p}{\lambda}} \cdot s_p}_{\text{Undesired Interference}} \\ &\quad + \underbrace{\mathbf{f}_l^{\mathrm{T}} \cdot \mathbf{D}_{\parallel,\mathrm{r}}^{\mathrm{H}} \cdot \mathbf{n}}_{\text{Noise}}, \end{aligned} \tag{13}$$

where $\Delta\mathbf{h}_p$ corresponds to the p-th column of $\Delta\mathbf{H}$ and $\mathbf{e}_l$ is the basis vector with the l-th element 1 and others 0.

Considering the dominant part of the filtered signal, the desired signal part has phase offset due to $\mathbf{f}_l^{\mathrm{T}} \cdot \Delta\mathbf{h}_l$ and $e^{j\frac{2\pi t_l}{\lambda}}$. However, the phase offset on the constellation plane can be compensated by a VPS in the third stage or a phase-locked loop during a training process. We have the phase shift ϕ_l in the third stage as

$$\phi_l = -\arctan\left\{\frac{\Im[(N + \mathbf{f}_l^{\mathrm{T}} \cdot \Delta\mathbf{h}_l) \cdot e^{j\frac{2\pi t_l}{\lambda}}]}{\Re[(N + \mathbf{f}_l^{\mathrm{T}} \cdot \Delta\mathbf{h}_l) \cdot e^{j\frac{2\pi t_l}{\lambda}}]}\right\}. \tag{14}$$

Therefore, the weighting matrix $\mathbf{W}$ is modeled as

$$\mathbf{W} = \mathbf{\Phi} \cdot \mathbf{H}_{\mathrm{o}}^{\mathrm{H}} \cdot \mathbf{D}_{\parallel,\mathrm{r}}^{\mathrm{H}}, \tag{15}$$

where $\mathbf{\Phi}$ is a diagonal matrix and given by $\mathbf{\Phi} = \mathrm{diag}\{e^{j\phi_1},\ e^{j\phi_2}, \cdots,\ e^{j\phi_N}\}$.

B. Successive Channel Equalization for Uniform Rectangular Array

In this part, we propose a two-stage fixed analog equalizing network that reduces the complexity significantly. If the transmit and receive arrays after projecting on a plane that is perpendicular to the transmit direction are two N-element parallel *uniform rectangular arrays* (URAs), there are N_{V} antennas having the same x_l or x_i and N_{H} antennas having the same y_l or y_i with $N = N_{\mathrm{V}} \cdot N_{\mathrm{H}}$. By examining Equation (5) and (6), the phase coupling matrix $\mathbf{H}_\perp$ can be further factorized into a Kronecker product of two phase coupling matrices of ULAs [5] as

$$\mathbf{H}_\perp = \mathbf{H}_{\mathrm{H}} \otimes \mathbf{H}_{\mathrm{V}}, \tag{16}$$

where $\otimes$ indicates Kronecker product operation. $\mathbf{H}_{\mathrm{H}}$ and $\mathbf{H}_{\mathrm{V}}$ denote two phase coupling matrices of ULAs with N_{H} and N_{V} elements respectively. In case of optimal arrangement, both $\mathbf{H}_{\mathrm{H}}$ and $\mathbf{H}_{\mathrm{V}}$ are orthogonal matrices. Therefore, we have $\mathbf{H}_\perp^{\mathrm{H}} \cdot \mathbf{H}_\perp = N \cdot \mathbf{I}_N$, $\mathbf{H}_{\mathrm{H}}^{\mathrm{H}} \cdot \mathbf{H}_{\mathrm{H}} = N_{\mathrm{H}} \cdot \mathbf{I}_{N_{\mathrm{H}}}$, and $\mathbf{H}_{\mathrm{V}}^{\mathrm{H}} \cdot \mathbf{H}_{\mathrm{V}} = N_{\mathrm{V}} \cdot \mathbf{I}_{N_{\mathrm{V}}}$.

Considering that the Hermitian operation is distributive over the Kronecker product [17], we have

$$\mathbf{H}_\perp^{\mathrm{H}} = \mathbf{H}_{\mathrm{H}}^{\mathrm{H}} \otimes \mathbf{H}_{\mathrm{V}}^{\mathrm{H}}. \tag{17}$$

Kronecker product operation in hardware design for a fixed network means a two-stage repetitive operation. The signals of each stage can be split into multiple subsets and each subset is applied with the same operation at this stage. Therefore, the design complexity reduces significantly. As shown in Fig. 6, instead of designing a fixed network with N^2 different paths between every input and output, the complexity is reduced to design two fixed networks with N_{H}^2 and N_{V}^2 different paths respectively. Furthermore, considering the required components in the proposed two-stage scheme, the required number of fixed phase shifters is reduced from $N^2 = N_{\mathrm{H}}^2 \cdot N_{\mathrm{V}}^2$ to $N_{\mathrm{H}}^2 \cdot N_{\mathrm{V}} + N_{\mathrm{V}}^2 \cdot N_{\mathrm{H}} = N_{\mathrm{H}} \cdot N_{\mathrm{V}} \cdot (N_{\mathrm{H}} + N_{\mathrm{V}})$. If $N_{\mathrm{H}} = N_{\mathrm{V}}$, the complexity reduces from $O(N_{\mathrm{V}}^4)$ to $O(N_{\mathrm{V}}^3)$.

Considering Equation (16), even if the arrangement is not optimal, the $\mathbf{H}_{\mathrm{H}}$, $\mathbf{H}_{\mathrm{V}}$ of parallel URAs are still invertible. Therefore, the inverse operation for a digital system is also distributive over the Kronecker product as

$$(\mathbf{H}_{\mathrm{H}} \otimes \mathbf{H}_{\mathrm{V}})^{-1} = \mathbf{H}_{\mathrm{H}}^{-1} \otimes \mathbf{H}_{\mathrm{V}}^{-1}. \tag{18}$$

If the computational complexity for inverse operation of a matrix with size $M \times M$ is $O(M^a)$, $a > 1$, the computational complexity reduces from $O(N^a)$ to $O(N_{\mathrm{H}}^a) + O(N_{\mathrm{H}}^a)$ considering that the complexity of Kronecker product is much smaller than matrix inverse operation.

IV. Mutual Information Analysis

Due to the fact that the displacement introduces undesired interferences to streams and in order to evaluate the performance, we use mutual information as our measure for the

performance evaluation. To compare the system with and without equalizing network, based on the receive vectors $\mathbf{y}$ and $\mathbf{y}_{\mathrm{W}}$ before and after equalization, we consider their respective quantized versions. The quantized receive vector $\mathbf{y}_{\mathrm{Q}}$ with b-bits ADCs is defined as

$$\mathbf{y}_{\mathrm{Q}} = \mathbf{Q}_b(\mathbf{y}), \tag{19}$$

while the $\mathbf{y}_{\mathrm{WQ}}$ follows the definition given in Section II.

The symbol $I_b(\mathbf{s};\mathbf{y}_{\mathrm{Q}})$ denotes the mutual information between the transmit vector and the receive vector quantized with b-bits defined in the standard way by a difference of unconditional and conditional entropy as

$$\begin{aligned} I_b(\mathbf{s};\mathbf{y}_{\mathrm{Q}}) &= H(\mathbf{y}_{\mathrm{Q}}) - H(\mathbf{y}_{\mathrm{Q}}|\mathbf{s}) \\ &= H(\mathbf{y}_{\mathrm{Q}}) - H\left[\mathbf{Q}_b(\mathbf{H}\cdot\mathbf{s}+\mathbf{n})|\mathbf{s}\right]. \end{aligned} \tag{20}$$

The mutual information $I_b(\mathbf{s},\mathbf{y}_{\mathrm{WQ}})$ between $\mathbf{s}$ and $\mathbf{y}_{\mathrm{WQ}}$ with ADC resolution of b-bits is expressed as

$$\begin{aligned} I_b(\mathbf{s};\mathbf{y}_{\mathrm{WQ}}) &= H(\mathbf{y}_{\mathrm{WQ}}) - H(\mathbf{y}_{\mathrm{WQ}}|\mathbf{s}) \\ &= H(\mathbf{y}_{\mathrm{WQ}}) - H\left[\mathbf{Q}_b(\mathbf{W}\cdot\mathbf{H}\cdot\mathbf{s}+\tilde{\mathbf{n}})|\mathbf{s}\right]. \end{aligned} \tag{21}$$

In the evaluation, we assume the channel matrix $\mathbf{H}$ to be perfectly known. Due to the non-linearity of the quantizing operation, the values of $H(\mathbf{y}_{\mathrm{WQ}}|\mathbf{s})$ and $H(\mathbf{y}_{\mathrm{Q}}|\mathbf{s})$ are difficult to evaluate. However, as we are focusing on the effects that are caused by using analog equalizing network and quantizers, we consider the noise-free case (high SNR limit) for which it holds that $H(\mathbf{y}_{\mathrm{WQ}}|\mathbf{s}) = H(\mathbf{y}_{\mathrm{Q}}|\mathbf{s}) = 0$. The analog equalizing network may reshape the distribution of the constellations on the complex constellation plane of every data stream before the quantization. Therefore a weighting matrix $\mathbf{W}$ is capable of increasing the entropy of the quantized vector $\mathbf{y}_{\mathrm{Q}}$ and making $H(\mathbf{y}_{\mathrm{WQ}}) \geq H(\mathbf{y}_{\mathrm{Q}})$. Considering Equation (20) and (21), the analog equalizing network can potentially generate $I_b(\mathbf{s};\mathbf{y}_{\mathrm{WQ}}) \geq I_b(\mathbf{s};\mathbf{y}_{\mathrm{Q}})$.

In Section V we compare the mutual information of the proposed system with N independent streams. Assuming that all possible transmit vectors have equal probabilities with $p_{\mathbf{s}}(\boldsymbol{\mathcal{S}}) = 1/|\mathbb{M}| = (1/K)^N$, $\boldsymbol{\mathcal{S}} \in \mathbb{M}$, the achievable rates of the system can be numerically evaluated as

$$R_{\mathrm{Q}} = I_b(\mathbf{s};\mathbf{y}_{\mathrm{Q}}),\ \text{s.t.}\ \forall\boldsymbol{\mathcal{S}},\ p_{\mathbf{s}}(\boldsymbol{\mathcal{S}}) = 1/|\mathbb{M}|, \tag{22}$$

$$R_{\mathrm{WQ}} = I_b(\mathbf{s};\mathbf{y}_{\mathrm{WQ}}),\ \text{s.t.}\ \forall\boldsymbol{\mathcal{S}},\ p_{\mathbf{s}}(\boldsymbol{\mathcal{S}}) = 1/|\mathbb{M}|. \tag{23}$$

V. Numerical Analysis on Robustness

To show the benefits of analog equalization, we use quantizers with the minimal required resolution matched to the cardinality of the modulation alphabet. When the channel is badly equalized, the desired signal is interfered by other signals. The corresponding quantizer faces a larger dynamic range from the superposition of multiple streams.

To illustrate the performance we evaluate the mutual information with and without equalization for $N = 3$ and $N = 4$ antennas of ULAs at transmitter and receiver side for 16-QAM modulation on all N streams. The quantization resolution was set to $b = 2$ bits using uniformly distributed quantization levels and a quantization range equal to the maximal possible magnitude of the receive symbols at the ADC inputs without noise. To study the behavior for a case of practical interest we picked the distance value $D = 100$ m and a carrier frequency of 60 GHz corresponding to a wireless backhaul scenario discussed in [2].

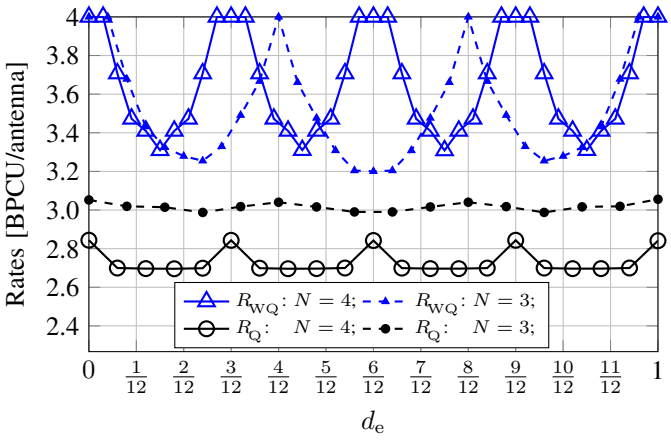

Fig. 7: Robustness of the system using fixed stream separation design. d_{e} is introduced via rotation error around x-axis.

The undesired interference in Equation (13) is caused by displacements of the antenna arrangement. As discussed before, the links will be more sensitive w.r.t. offset *differences* along the transmit direction. To evaluate the impact of these offset differences, we examine the mutual information with displaced antennas in the zero noise case for rotations around the x-axis (see the sketch in Fig. 1). This x-axis rotation error may arise in a practical system due to displacements during manufacturing and/or installation and/or wind pressure.

Having a rotation error θ around the x-axis, the receive antenna offsets r_i with $1 \leq i \leq N$ can be expressed as $r_i = (2i-N-1)/2 \cdot d_{\mathrm{V}} \cdot \sin\theta$ assuming that the z-axis passes through the phase center of the transceiver arrays. Therefore, the offset between the neighbor elements has an offset difference of $d_{\mathrm{V}} \cdot \sin\theta$. Due to the fact that the offset differences are scaled by the wavelength as $1/\lambda$, we write the error introduced by the angle θ in a normalized form as $d_{\mathrm{e}} \triangleq d_{\mathrm{V}} \cdot \sin\theta/\lambda$. Because $d_{\mathrm{V}} \gg \lambda$, a small value θ is able to introduce a large d_{e}.

The sensitivity of the rates R_{WQ} and R_{Q} obtained from the evaluation of Equation (22) and (23) can be found in Fig. 7. The transmit rates are normalized with respect to the number of antenna pairs N. It is seen that the mutual information R_{WQ} achieves the maximum rate of 4 bits per stream while R_{Q} attains only about 75% of it for this particular case. In addition, the equalized system is rather sensitive to z-displacements while the unequalized system is not. Note, however, that the performance of the unequalized system could also be improved, if we would increase the number of quantization bits.

Furthermore, the performance periodically decrease and increase with a period $d_{\mathrm{e}} = 1$ as expected. However, an interesting finding is that an additional smaller d_{e} period that

are multiples of $1/N$ is observed. This is because that the equalized channels $\mathbf{H}_{\mathrm{o}}^{\mathrm{H}} \cdot \mathbf{H}$ are no longer corresponding to effective identity matrices but to permutation matrices that permute the data streams. Therefore, there is no information loss.

It is interesting to explain the observations reported in [12], [13], [14], with the described sensitivity of spatial multiplexing over an approximately orthogonal LoS channel. In those works, a relative displacement in the millimeter range can be easily found. Therefore, an adaption loop was introduced in order to adjust the gains and phases for equalization and stream separation at the receiver side.

Let us also note that the proposed analog equalization scheme with reduced complexity in the analog RF front-end appears as robust against displacements of the antennas within the array plane as reported in [5]. More details of the robustness can be found in our work [16]. The benefits of analog equalization may be fully exploited even with large displacement range in the link direction, if the z-displacements of the antennas at transmitter and receiver side can be estimated and compensated by phase shifters as indicated in Fig 5.

VI. Conclusion

In this paper, we examined transmission over an approximately orthogonal LoS MIMO-channel with digital and hybrid analog/digital receiver processing. We firstly identified different sensitivities for relative displacements of the antennas along the link direction and in the plane(s) of the arrays. We proposed an analog equalization (stream separation) scheme to be implemented in the RF front-end to reduce the dynamic of the signals and to save power/computing efforts. In addition to fixed analog equalizing networks, the scheme uses an adaptation loop that adjusts phase errors. The scheme makes the system robust w.r.t. relative displacements along the link direction. Without additional adaptation loop, fixed analog equalizing networks are very sensitive to displacement errors as shown by our numerical analysis. Finally, as the LoS channel matrix of rectangular arrays can be factored into a Kronecker product, other simplifications on fixed analog equalizing network design and digital processing were outlined. The whole design significantly reduces cost and complexity compared to a digital implementation of the required filtering at the receiver side.

References

[1] G. Fettweis, "LTE: The Move to Global Cellular Broadband," *Intel Technical Journal, special issue on LTE*, vol. 18, pp. 7–10, Feb 2014.

[2] X. Song, C. Jans, L. Landau, D. Cvetkovski, and G. Fettweis, "A 60GHz LOS MIMO Backhaul Design Combining Spatial Multiplexing and Beamforming for a 100Gbps Throughput," in *Proceedings of the IEEE Global Communications Conference*, Dec 2015.

[3] D. Gesbert, H. Bolcskei, D. Gore, and A. Paulraj, "Outdoor MIMO Wireless Channels: Models and Performance Prediction," *IEEE Transactions on Communications*, vol. 50, no. 12, pp. 1926–1934, Dec 2002.

[4] T. Haustein and U. Kruger, "Smart Geometrical Antenna Design Exploiting the LOS Component to Enhance a MIMO System Based on Rayleigh-fading in Indoor Scenarios," in *Proceedings of the 14th IEEE Proceedings on Personal, Indoor and Mobile Radio Communications*, vol. 2, Sept 2003, pp. 1144–1148.

[5] P. Larsson, "Lattice Array Receiver and Sender for Spatially Orthonormal MIMO Communication," in *Proceedings of the IEEE 61st Vehicular Technology Conference*, vol. 1, May 2005, pp. 192–196.

[6] F. Bohagen, P. Orten, and G. Oien, "Construction and Capacity Analysis of High-rank Line-of-sight MIMO Channels," in *Proceedings of the IEEE Wireless Communications and Networking Conference*, vol. 1, March 2005, pp. 432–437.

[7] ——, "Optimal Design of Uniform Planar Antenna Arrays for Strong Line-of-Sight MIMO Channels," in *Proceedings of the IEEE 7th Workshop on Signal Processing Advances in Wireless Communications*, July 2006, pp. 1–5.

[8] C. Zhou, X. Chen, X. Zhang, S. Zhou, M. Zhao, and J. Wang, "Antenna Array Design for LOS-MIMO and Gigabit Ethernet Switch-Based Gbps Radio System," *International Journal of Antennas and Propagation*, 2012.

[9] X. Song and G. Fettweis, "On Spatial Multiplexing of Strong Line-of-Sight MIMO With 3D Antenna Arrangements," *IEEE Wireless Communications Letters*, vol. 4, no. 4, pp. 393–396, Aug 2015.

[10] K. Hiraga, K. Sakamoto, T. Seki, T. Nakagawa, and K. Uehara, "Effects of Weight Errors on Capacity in Simple Decoding of Short-Range MIMO Transmission," *IEICE Communications Express*, vol. 2, no. 5, pp. 193–199, 2013.

[11] K. Hiraga, K. Sakamoto, T. Seki, T. Tsubaki, H. Toshinaga, and T. Nakagawa, "Performance Measurement of Broadband Simple Decoding in Short-Range MIMO," in *Proceedings of the IEEE International Symposium on Personal, Indoor and Mobile Radio Communications*, Sept 2014, pp. 213–216.

[12] C. Sheldon, E. Torkildson, M. Seo, C. Yue, U. Madhow, and M. Rodwell, "A 60GHz Line-of-sight 2x2 MIMO Link Operating at 1.2Gbps," in *Proceedings of the IEEE International Antennas and Propagation Society Symposium*, July 2008.

[13] C. Sheldon, E. Torkildson, M. Seo, C. Yue, M. Rodwell, and U. Madhow, "Spatial Multiplexing over a Line-of-Sight Millimeter-wave MIMO Link: A Two-Channel Hardware Demonstration at 1.2Gbps over 41m Range," in *Proceedings of European Conference on Wireless Technology*, Oct 2008, pp. 198–201.

[14] C. Sheldon, M. Seo, E. Torkildson, M. Rodwell, and U. Madhow, "Four-channel Spatial Multiplexing over a Millimeter-Wave Line-of-Sight Link," in *Proceedings of the IEEE MTT-S International Microwave Symposium Digest*, June 2009, pp. 389–392.

[15] T. LaRocca, J. Liu, F. Wang, and F. Chang, "Embedded DiCAD Linear Phase Shifter for 57-65GHz Reconfigurable Direct Frequency Modulation in 90nm CMOS," in *Proceedings of the IEEE Radio Frequency Integrated Circuits Symposium*, June 2009, pp. 219–222.

[16] X. Song, T. Haelsig, W. Rave, B. Lankl, and G. Fettweis, "Analog Equalization and Low Resolution Quantization in Strong Line-of-Sight MIMO Communication," in *Proceedings of IEEE International Conference on Communications*, May 2016.

[17] C. F. Loan, "The Ubiquitous Kronecker Product ," *Journal of Computational and Applied Mathematics*, vol. 123, no. 12, pp. 85 – 100, 2000.